the fusion assay (curve B) at 10 °C are shown in Figure 17. The results clearly indicate that the fusion process does take place with the DMPC vesicles. The process was further accelerated upon addition of calcium ions ($CaCl_2$)[8c,20] (curve C in Figure 17).

Concluding Remarks

As listed in Table VI, all the physical parameters for single-walled vesicles of $N^+C_5Ala2C_{16}$ and egg lecithin are comparable to each other. In other words, the physical shape and amphiphile aggregation mode of the vesicles of peptide amphiphiles are nearly identical with those of the vesicles of naturally occurring phospholipids having aliphatic double chains of comparable sizes. However, the single-walled vesicles formed with the former amphiphiles are structurally much more stable than those with the latter and stay in solution over at least a month without meaningful morphological change. Such structural stability seems to originate in the formation of stronger hydrogen-belt domains through intravesicular hydrogen-bonding interaction between the amino acid residues. The present amphiphiles do not undergo hydrolysis even in acidic and alkaline media at room temperature for a reasonably prolonged period of time, while diacylphosphatiylcholines are readily decomposed under the same conditions.

Even though the intervesicular exchange of the amphiphile molecules takes place between the single-walled vesicles via a collision mechanism, they do not undergo fusion to form larger aggregates in a reasonably prolonged period of time. Permeability of charged water-soluble materials across the bilayer membrane is extremely sluggish and nearly inhibited at temperatures below T_m. The present results suggest that these peptide amphiphiles have great potential to become effective drug carriers in the state of single-walled vesicles.

Acknowledgment. The present work was supported in part by a Grant-in-Aid for Scientific Research from the Ministry of Education, Science and Culture of Japan (No. 58430016).

Registry No. DMPC, 18194-24-6; SP, 89637-61-6; SP-$N^+C_5Ala2C_{16}$, 89637-60-5; $N^+C_5Ala2C_8$, 89637-54-7; $N^+C_5Ala2C_{10}$, 89637-55-8; $N^+C_5Ala2C_{12}$, 78761-16-7; $N^+C_5Ala2C_{14}$, 83825-02-9; $N^+C_5Ala2C_{16}$, 88598-40-7; $N^+C_5Ala2C_{18}$, 89637-56-9; $N^+C_2Ala2C_{16}$, 89637-57-0; $N^+C_7Ala2C_{16}$, 89637-58-1; $N^+C_{10}Ala2C_{16}$, 89637-59-2; $2C_1NC_5Ala2C_{16}$, 89637-62-7; *N*-(1-oxyl-2,2,6,6-tetramethyl-4-piperidyl)iodoacetamide, 25713-24-0; ascorbic acid, 50-81-7.

Quantum Mechanical and Molecular Mechanical Studies on a Model for the Dihydroxyacetone Phosphate–Glyceraldehyde Phosphate Isomerization Catalyzed by Triosephosphate Isomerase (TIM)

Giuliano Alagona,† Peter Desmeules, Caterina Ghio,† and Peter A. Kollman*

Contribution from the Department of Pharmaceutical Chemistry, School of Pharmacy, University of California, San Francisco, California 94143. *Received July 13, 1983*

Abstract: We have carried out ab initio (SCF + MP2) and molecular mechanical calculations on a model for the reaction catalyzed by triosephosphate isomerase. To our knowledge, this is the first time that ab initio SCF, correlation energy, and environmental effect calculations have been carried out on all the chemical steps of an enzymatic reaction, along with molecular mechanical simulation of some steps. The quantum mechanical calculations show how the TIM-catalyzed reaction, one of the most efficient known, can have as its rate-limiting step product dissociation in that the effect of the enzyme is to make the *chemical* steps very rapid. The enzyme does this by stabilizing the enzyme–intermediate complex so that it becomes of approximately equal stability to the enzyme–substrate complex. This lowers the barrier between these species to the range of 10–15 kcal/mol. The molecular mechanical calculations have been used to generate refined coordinates for the enzyme–substrate and enzyme–intermediate complexes, which were essential in evaluating environmental effects on the quantum mechanical energies. They have also been used to suggest the effect of genetic mutation of the key active site histidine residue in TIM to a glutamine. Our calculations suggest the chemical steps in this mutant TIM will be less effective than in the normal enzyme, for reasons which had not been suggested heretofore.

One of the most efficient enzyme-catalyzed reactions is the triosephosphate isomerase (TIM) catalyzed reversible isomerization of dihydroxyacetone phosphate (DHAP) to glyceraldehyde 3-phosphate (GAP). In an elegant set of papers, using isotope labeling and kinetic methods, Knowles and co-workers[1] determined a complete free energy profile for the enzyme-catalyzed reaction and suggested that this enzyme was "perfectly evolved" in that the rate-determining step for the DHAP ⇌ GAP isomerization was product dissociation from the enzyme. Thus, there is no evolutionary pressure for the enzyme to improve the catalytic efficiency of the reactive steps on the enzyme. The enzyme-catalyzed reaction of TIM should be a very interesting one to study in that it should give us insight into how the enzyme achieves its enormous catalytic rate enhancement (10^9 over the uncatalyzed reaction). The mechanism of the TIM-catalyzed reaction is reasonably well understood (Schemes I and II).

Scheme I

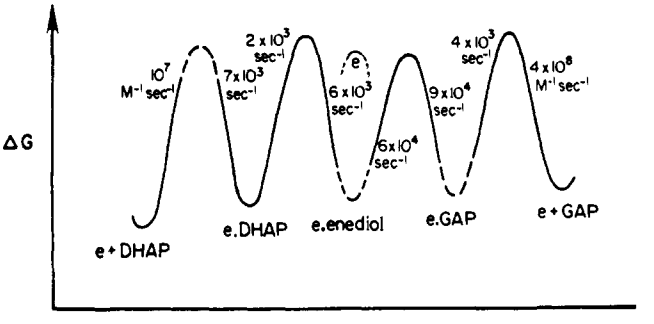

Scheme I details the free energy profile suggested by Knowles et al.,[1] in which there are five species: e + DHAP (separated enzyme + dihydroxyacetone phosphate), e·DHAP (Michaelis

† Permanent address: Istituto di Chimica Quantistica ed Energetica Molecolare del C.N.R., Pisa, Italy.

(1) Leadlay, P. F.; Albery, W. J.; Knowles, J. R. *Biochemistry* **1976**, *15*, 5617. Albery, W. J.; Knowles, J. R. *Ibid.* **1976**, *15*, 5588, 5627.

0002-7863/84/1506-3623$01.50/0

Scheme II

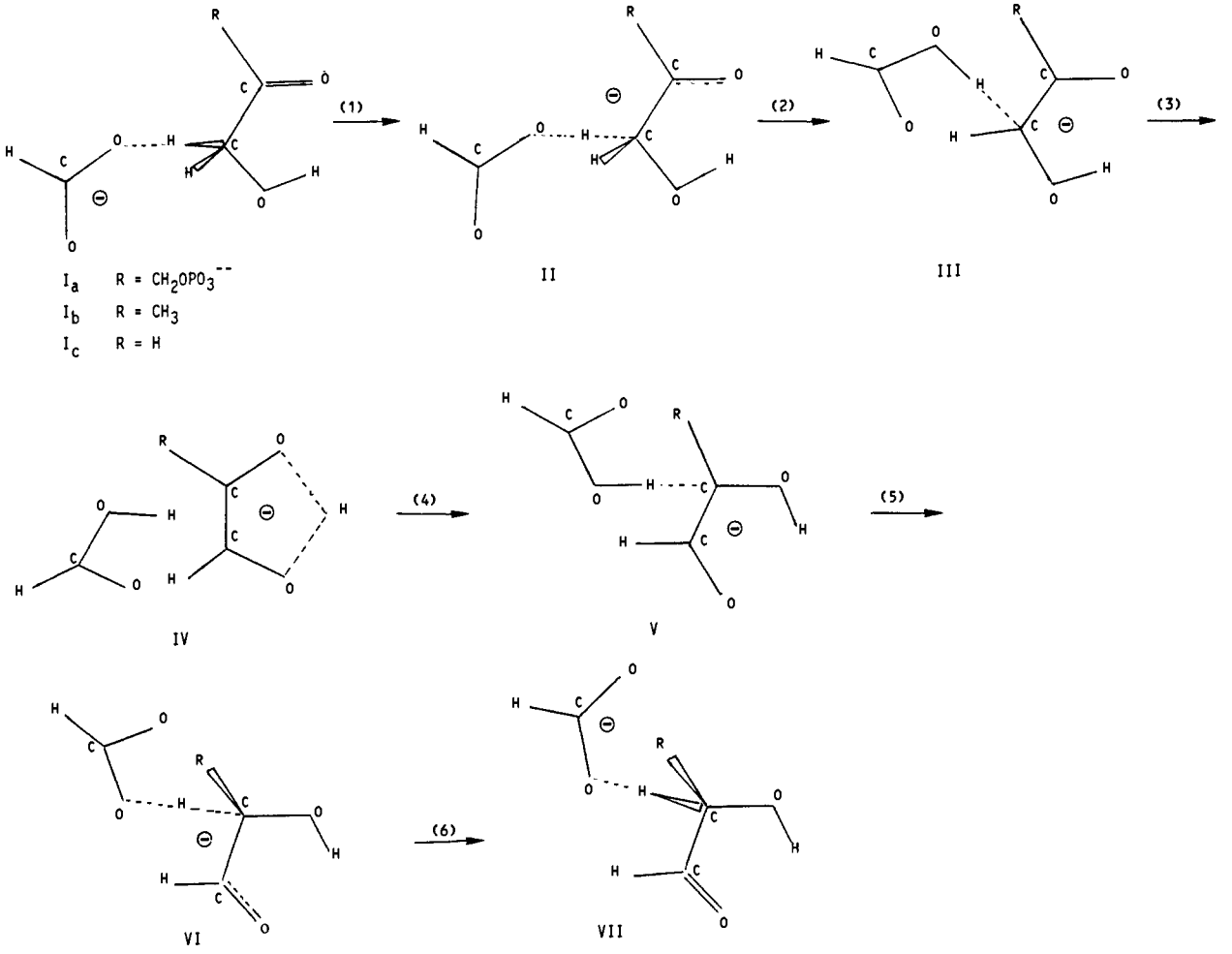

complex of these two species), e·enediol (enzyme enediol(ate) intermediate complex), e·GAP (enzyme–product (glyceraldehyde 3-phosphate) Michaelis complex), and e + GAP (separated enzyme and product). There are four steps connecting these five species. The first and last are noncovalent steps involving enzyme–substrate (product) Michaelis complex formations. Scheme II elaborates on the *chemical* steps between the second and third species in Scheme I; the chemical steps between the third and fourth species are analogous to these.

What is known about these *chemical* steps? Studies by Rose and co-workers[2] suggested that a base on the enzyme abstracts a C–H hydrogen from the *re* face of the C_1 carbon of DHAP and delivers a proton back to C_2 to form GAP. Knowles et al.[1] later showed that significant loss of label occurred during this isomerization. Subsequent X-ray studies by Banner et al.[3] and Alber and Petsko[4] have established this base as Glu 165 in both chicken muscle and yeast TIM. Even in the presence of a base, the question remained how a carboxylate group ($pK_a \sim 4$) could abstract a C–H proton from DHAP ($pK_a \sim 14$) so easily. Thus Knowles suggested[5] a polarizing electrophile in the active site of TIM which could stabilize the incipient anion. The X-ray structural studies[3] suggested that this electrophile was either or both His 95 and Lys 13. The earlier studies of the TIM-catalyzed reaction suggested that there was an intermediate enediolate anion to which a proton could be delivered to form either DHAP or GAP. Subsequent studies[6] have suggested the intermediate is an enediol rather than an enediolate, but the nature of the intermediate has not been definitively established. Although the X-ray structure of TIM and its DHAP complex[3,4] is not as highly refined as some, its accuracy is sufficient for our present purposes, and it is likely that improvements in the structural analysis will continue.

Even more exciting is the prospect of using recombinant DNA techniques to create modified enzymes and to combine experimental studies on such enzymes with theoretical calculations. Recently, Alber and Kawasaki and Davenport and Petsko[7] have cloned the yeast TIM gene and are working on the expression of mutant genes with selected amino acid substitutions.

There have been a large number of model quantum mechanical studies of enzyme-catalyzed reactions. The serine proteases have received considerable attention, both at the semiempirical[8] and at the ab initio[9] levels. In only one study, however, was an ex-

(2) Rieder, S. V.; Rose, I. A. *J. Biol. Chem.* **1959**, *234*, 10007. Rose, I. A. *Brookhaven Symp. Biol.* **1962**, *15*, 293.
(3) Banner, D. W.; Bloomer, A. C.; Petsko, G. A.; Phillips, D. C.; Pogson, C. I. *Cold Spring Harbor Symp. Quant. Biol.* **1971**, *36*, 151. Banner, D. W.; Bloomer, A. C.; Petsko, G. A.; Phillips, D. C.; Pogson, C. I.; Wilson, I. A. *Nature (London)* **1975**, *255*, 609.
(4) Alber, T.; Petsko, G. *J. Mol. Biol.* submitted for publication. Alber, T.; Petsko, G. *Biochemistry*, submitted for publication.
(5) Knowles, J. *Acc. Chem. Res.* **1977**, *10*, 105.
(6) Iyengar, R.; Rose, I. *Biochemistry* **1981**, *20*, 1223, 1229.
(7) Alber, T.; Kawasaki, G. *J. Mol. Appl. Genet.*, in press. Davenport, R.; Petsko, G., unpublished data.
(8) (a) Scheiner, S.; Kleier, D.; Lipscomb, W. *Proc. Natl. Acad. Sci. U.S.A.* **1975**, *72*, 2606. Scheiner, S.; Lipscomb, W. *Ibid.* **1976**, *73*, 432. (b) Umeyama, H.; Imamura, A.; Nagata, C.; Hanano, M. *J. Theor. Biol.* **1973**, *41*, 485. Amidon, G. *Ibid.* **1974**, *46*, 101. Kitayama, H.; Fukutome, H. *Ibid.* **1976**, *60*, 1. Beppu, Y.; Yomosa, S. *J. Phys. Soc. Jpn.* **1977**, *42*, 1694.
(9) Hayes, D.; Kollman, P. In "Catalysis in Chemistry and Biochemistry: Theory and Experiment"; Pullman, B., Ed.; Reidel: Boston, 1979; p 77. Umeyama, H.; Nakagawa, S. *Chem. Pharm. Bull.* **1979**, *27*, 1524. Nakagawa, S.; Umeyama, H.; Kudo, T. *Ibid.* **1980**, *28*, 1342. Kollman, P.; Hayes, D. M. *J. Am. Chem. Soc.* **1981**, *101*, 2955. Umeyama, H.; Nakagawa, S.; Kudo, T. *J. Mol. Biol.* **1981**, *150*, 409. Umeyama, H.; Nakagawa, S. *Chem. Pharm. Bull.* **1982**, *30*, 2252; *J. Theor. Biol.* **1982**, *99*, 759. Nakagawa, S.; Umeyama, H. *FEBS Lett.* **1982**, *139*, 181; *Bioorg. Chem.* **1982**, *11*, 322. Allen, L. C. *Ann. N.Y. Acad. Sci.* **1981**, *367*, 383.

tensive analysis of the potential surface for the enzyme-catalyzed reaction carried out.[8a] Ribonuclease,[10] papain,[11] liver alcohol dehydrogenase,[12] carboxypeptidase,[13] and carbonic anhydrase[14] catalyzed reactions have also received attention from theoreticians. However, with the exception of carbonic anhydrase, the reaction mechanisms for the remaining systems involved charge separation during the reaction pathway, which is especially difficult to model in a semiquantitative fashion. For example, in the serine proteases, it is likely that a His–Ser–substrate complex becomes $HisH^+$–Ser–$substrate^-$ species in the transition state of the reaction.[15] The carbonic anhydrase reaction probably does not involve charge separation but contains a ligated Zn^{2+} ion, which is more difficult to model precisely by currently available quantum mechanical methods. The TIM-catalyzed reaction is especially attractive in this regard in that it involves merely the transfer of an anionic charge from enzyme to substrate back to enzyme, with no necessity for charge separation.

There have also been important technical developments in recent years which made the study described below reasonable. The incorporation of a "routine" and systematic method of calculating correlation energies has been accomplished in the landmark ab initio program GAUSSIAN 80.[16] This enables a *reasonable* estimate of the energy for bond-breaking reactions by ab initio quantum mechanical methods. The combined use of (stereo) computer graphics and molecular mechanics[17,18] also has been important in helping one model and understand complex, multiatom systems.

Given improvements in theoretical methodologies, we are in a position to apply quantum mechanical and molecular mechanical methods to the TIM-catalyzed reaction.[19] Below we proceed as follows, asking four questions. First, what is the *intrinsic* energy required for the abstraction of the C–H proton of DHAP by the carboxylate base of glutamate? The answer to this is ~25 kcal/mol. Such an energy difference is completely inconsistent with the low barriers between species e·DHAP, e·enediol, and e·GAP and their approximately equal energies. Second, how does the enzyme change this intrinsic energy? Our molecular mechanical and quantum mechanical calculations concur that, if one appropriately solvates the PO_3^{2-} part of the substrate, His 95 and the Lys 13–Glu 97 ion pair of the enzyme stabilize the enzyme–enediolate complex sufficiently to change the intrinsic energy for C–H proton abstraction to approximately zero. Third, what are the proton-transfer barriers of steps 2 and 3 of Scheme I (steps 1–2 and 5–6 of Scheme II)? Here we turn to model systems that have similar energies before and after proton transfer and find that, if the C···O distance is <3.0 Å, the proton transfer barrier is <10 kcal/mol. We also use the molecular mechanics calculations to show that such a geometry costs little "strain" energy to achieve. Calculations on the isomerization of the enediolate (steps 3 and 4 in Scheme II) show the barrier there to be ~10–15 kcal/mol as well.

Given the importance of His 95 in stabilizing e·enediol and lowering the barrier to proton transfer in TIM, the final question asked is: what are the consequences of changing this His to Gln, as is being done experimentally by Davenport and Petsko?[7] The quantum mechanical calculations suggest that if Gln 95 is located where His 95 is, it should be almost as effective at promoting proton transfer. The molecular mechanical calculations, on the other hand, suggest a "conformational change" of Gln 95, which could make it less effective at facilitating proton transfer.

Methods

Initially, we optimized the ab initio SCF energy of α-hydroxyacetone and its enediolate anion by using an STO-3G basis set and the gradient optimization algorithm in the program AKSCF, available from the National Resource in Computational Chemistry.[22] These calculations were carried out by P.D. on the LBL CDC 7600. Subsequently we partially refined these molecules at the 4-31G level by using cyclical optimization. These and all the remaining calculations were carried out by the other authors using the program GAUSSIAN 80 UCSF.[23] This program is an enhanced version of the program GAUSSIAN 80 developed by Pople and co-workers.[16] All these ab initio calculations were carried out on the UCSF Structural Biology VMS VAX 11/780. The molecular mechanical calculations used the program AMBER,[24] running on the VAX. Earlier calculations used the chicken muscle TIM coordinates,[3] and later ones used the yeast TIM (YTIM) coordinates of Alber and Petsko.[4] We used the qualitative features of the TIM–DHAP complex[7] to identify those residues within 8 Å of any atom of DHAP, and only these residues were included in the subsequent molecular mechanical refinement. As previously,[18] we restrained all Cα carbons at the termini of the chains with a 10 kcal/(mol Å^2) penalty function. Such calculations followed computer model building using the program CHEM,[25] running on the computer Graphics Lab VAX 11/750 and Evans and Sutherland color picture system 2. These molecular mechanical calculations[26] followed closely the procedure in ref 18

(10) Deakyne, C.; Allen, L. C. *J. Am. Chem. Soc.* **1979**, *101*, 3951.
(11) van Duijnen, P.; Thole, B.; Hol, W. *Biophys. J.* **1979**, *9*, 273. van Duijnen, P.; Thole, B.; Broer, B.; Niewpoort, W. *Int. J. Quantum Chem.*, in press. Clementi, E. *Ibid.* **1980**, *17*, 651.
(12) Sheridan, R.; Deakyne, C.; Allen, L. C. In "Advances in Experimental Medicine and Biology. Proceedings of the Third International Symposium on Alcohol and Aldehyde Metabolizing Systems"; Thurman, R. G., Ed.; Plenum Press: New York, 1980; pp 705–713.
(13) Hayes, D. M.; Kollman, P. *J. Am. Chem. Soc.* **1976**, *98*, 7811. Osman, R.; Weinstein, H. *Isr. J. Chem.* **1980**, *19*, 149. Topiol, S.; Osman, R.; Weinstein, H. *Ann. N.Y. Acad. Sci.* **1981**, *367*, 17.
(14) Demoulin, D.; Pullman, A.; Sarkar, B. *J. Am. Chem. Soc.* **1977**, *99*, 8498. Demoulin, D.; Pullman, A. *Theor. Chim. Acta* **1978**, *49*, 161. Demoulin, D.; Pullman, A. In "Catalysis in Chemistry and Biochemistry, Theory and Experiment, 12th Jerusalem Symposium"; Pullman, B., Ed.; Reidel: Dordecht, 1979; pp 51–66. Sheridan, R.; Allen, L. C. *J. Am. Chem. Soc.* **1981**, *103*, 1544. Allen, L. C. *Ann. N.Y. Acad. Sci.* **1981**, *367*, 383.
(15) Kosiakoff, A.; Spencer, S. *Nature (London)* **1980**, *288*, 414.
(16) Whiteside, R.; Krishman, R.; Seegar, R.; De Frees, D.; Schlegel, H.; Binkley, J.; Topiol, S.; Kahn, J.; Pople, J. GAUSSIAN 80, QCPE Program No. 406.
(17) Blaney, J.; Weiner, P.; Dearing, A.; Kollman, P.; Jorgensen, E. C.; Oatley, S.; Burridge, J.; Blake, C. C. F. *J. Am. Chem. Soc.* **1982**, *104*, 6424.
(18) Wipff, G.; Dearing, A.; Weiner, P.; Blaney, J.; Kollman, P. *J. Am. Chem. Soc.* **1983**, *105*, 997.
(19) To our knowledge, this is the first attempt to use both ab initio quantum mechanical and molecular mechanical methods to examine the chemical steps of an enzyme-catalyzed reaction. The only other ab initio quantum mechanical + molecular mechanical study of which we are aware of is that by Clementi,[20] but the focus there was on the ionic state of the His···Cys H bond and not on the subsequent enzymatic reaction. Combined quantum/molecular mechanical studies have been carried out by Warshel,[21] using either MINDO/2 or valence bond quantum mechanical methods, combined with a point dipole model of water and a molecular mechanical model of lysozyme. The focus was to demonstrate that the electrostatic stabilization of the protonated sugar transition state due to the two Glu residues in the enzyme is significantly greater than one finds in aqueous solution. Our model employs a more accurate level of quantum mechanical theory than those of Warshel et al.[21] but does not have as realistic a representation of the aqueous solution.
(20) Clementi, E. *Int. J. Quantum Chem.* **1980**, *17*, 651.
(21) Warshel, A. *J. Phys. Chem.* **1979**, *83*, 1646. Warshel, A.; Weiss, R. *J. Am. Chem. Soc.* **1980**, *102*, 6218.
(22) The program AKSCF was made available by the National Resource in Computation Chemistry (NRCC), and P.A.K. and P.D. would like to thank M. Dupuis and D. Spangler for its use.
(23) Singh, U. C.; Kollman, P. A. *QCPE*, **1982**, Bull. No. 2, Program No. 446.
(24) Weiner, P.; Kollman, P. *J. Comput. Chem.* **1981**, *2*, 287.
(25) CHEM, a program for molecular manipulation on the Evans and Sutherland Picture System 2, written by A. Dearing at UCSF.
(26) The molecular mechanical parameters for the protein came from: Weiner, S. J.; Kollman, P. A.; Case, D.; Singh, U. C.; Ghio, C.; Alagona, G.; Weiner, P. *J. Am. Chem. Soc.*, in press. For DHAP and the enediolate, we used the corresponding parameters for proteins or nucleic acid described in that paper where possible (e.g., for DHAP, the parameters for the alcohol group) but modified these in the following way: The partial charges for all but the non-phosphate came from Mulliken populations of the STO-3G calculations; for the phosphate group a net charge of 2– was used, one-third of which was assigned to each anionic oxygen molecule. In DHAP, a torsional potential was included to ensure that the conformation with H or O eclipsing the carbonyl oxygen was more favorable by 1 kcal/mol. The carbonyl oxygen was given a stretching force constant of 777 kcal/(mol Å^2); many of the other bond length and angle parameters came from the ab initio optimized geometries. For the enediolate anion, we used a value of 600 kcal/(mol Å^2) for the C_2–O^- and C_1–C_2 bonds and torsional barriers of 30 kcal/mol for these bonds; this value is half-way between the pure single and double bond values for the torsional barriers in ethylene. These values are reasonable, but will be further refined in the near future.

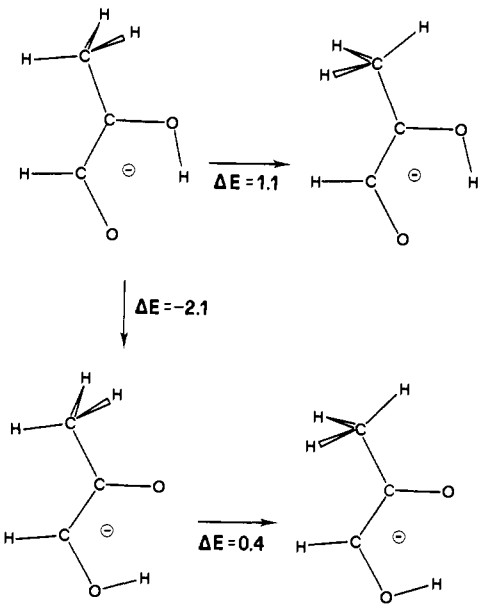

Figure 1. Relative energies of different conformations/isomers of III (R = CH_3) in kcal/mol, at the STO-3G level.

and were performed to give us qualitatively reasonable locations for the enzyme active site groups relative to the substrate. These locations and appropriate partial charges of the atoms were then used in the quantum mechanical calculations, as we have done previously in our studies of carboxypeptidase.[13]

Results

Quantum Mechanical Models. As noted above, Scheme II details the first chemical step of the TIM-catalyzed reaction, involving proton abstraction from DHAP (I) by a $-COO^-$ group of the enzyme to form the enediolate ion (IIIa) (steps 1–2), proton shuttling within the enediolate (steps 3–4), and proton transfer back to the substrate (steps 5–6). In our quantum mechanical calculations, we replaced the R = $CH_2OPO_3^{2-}$ (Ia) group with R = CH_3 (Ib) for most studies, although in a few cases we used R = H (Ic). From the point of view of electronic structure, this is a good assumption, since the $-CH_2-$ group has been found to be a good insulator between polar and ionic groups.[13] We used HCO_2^- as a model for the base (Glu 165). We began with a complete geometrical optimization of the α-hydroxyacetone (Ib, R = CH_3) and its enediolate anion (IIIb). The structure and energies of these are presented in Tables I and II along with the model for GAP (VII, R = CH_3) built from the optimized structure of I and then partially optimized (Table III). We already had STO-3G optimized geometries for $HCOO^-$ and HCOOH;[27] 4-31G optimized geometries of these are reported in Table IV. (Tables I–IV are included in the supplementary material, but the total energies are summarized in ref 28.) The geometrical parameters for these molecules are reasonable and contain no unusual features, but to our knowledge, this is the first reported calculation on enediolate anion (III), and its STO-3G calculated energy and conformational preferences are perhaps worthy of comment (see Figure 1). Not surprisingly, the isomer with the CH_3 next to $C-O^-$ is more stable than the isomer with the CH_3 next to the OH by 2.1 kcal/mol, since a methyl group can inductively stabilize a negative charge. The rotational barrier of CH_3 when it is next to the COH group is very similar to that found in methanol, with the "staggered" conformation more stable than the eclipsed by 1.1 kcal/mol. Interestingly, the CH_3 bound to the C–O is more stable when staggered with respect to the CO than eclipsed (albeit only by 0.4 kcal/mol). This is in contrast to the conformational preferences expected for a ketone, where the C–H would eclipse the C–O.

It is reasonable that the ketone (Ib) model for DHAP is calculated to be more stable than the aldehyde (VIIb) model for GAP by 5.9 kcal/mol at the 4-31G level; this is qualitatively consistent with the experimental[1] free energy difference between unhydrated DHAP and GAP of 3.3 kcal/mol, favoring DHAP.

Steps 1 and 2—the Relative Energy of I and III. We used model systems (see supplementary material, Table V) to determine appropriate C···O distances to use in our analysis of the energies of species I and III. These turned out to be 3.53 Å (4-31G) and 2.82 Å (STO-3G) for $HCOO^-$···DHAP (I) and 3.29 Å (4-31G) and 3.02 Å STO-3G for HCOOH···enediolate (III). We also needed appropriate geometrical parameters for a model of the transition state (II) for proton transfer, and, for II, we used linearly interpolated C···O distances. These parameters[29] are described

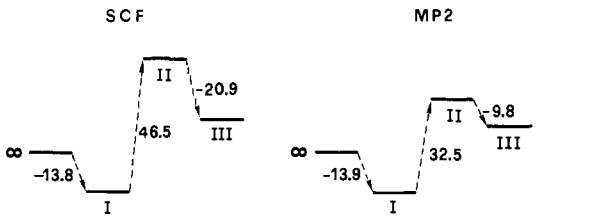

Figure 2. Relative energies of 4-31G model at the SCF and MP2 levels for I, II, and III with R = H.

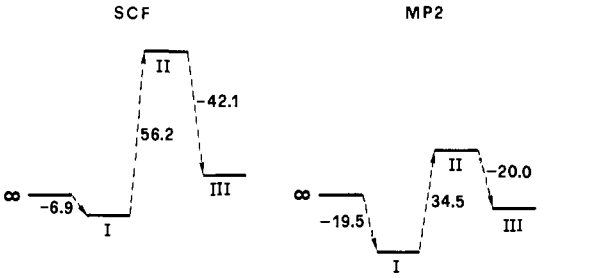

Figure 3. Relative energies of STO-3G model at the SCF and MP2 levels for I, II, and III with R = CH_3 at 4-31G minima.

Table VII. Energy for Proton Transfer as a Function of R(C···O) and % Proton Transfer[a,b]

R(C···O)	% proton transfer[d]	ΔE
3.415[c]	0	−14.4
3.1[c]	0	−15.1
2.9[c]	0	−13.9
3.415	50	34.9
3.1	50	17.6
2.9	50	9.5
2.7	50	5.6
2.5	50	9.1
2.9[c]	100	12.0
3.1[c]	100	11.5
3.415[c]	100	12.4

[a] Used HCOO···H···CHOHCHO model, geometry in supplementary material Table VI except as noted; all calculations used 4-31G basis set. [b] Energy in kcal/mol relative to isolated $HCOO^-$ and CH_2O-HCH. [c] Geometry in supplementary material Tables I, II, and IV. [d] R(C–H) = 1.1 Å = 0% proton transfer; R(O–H) = 1.0 Å = 100% proton transfer.

(27) These geometries come from: Kollman, P.; Hayes, D. *J. Am. Chem. Soc.* **1981**, *101*, 2955.

(28) For Ib, the STO-3G energy at the STO-3G optimized geometry is −263.3619 au; the 4-31G energy at the 4-31G optimized geometry is −266.41706 au. For enediolate (IIIb), the corresponding values are −262.57218 au (STO-3G) and −265.79712 au (4-31G). For aldehyde (VIIb), the corresponding energies are −263.35159 (STO-3G) and −266.40768 au (4-31G). For $HCOO^-$ and HCOOH, at the 4-31G optimized geometry, the energies are as follows: $HCOO^-$ (STO-3G–SCF) −185.45454, (MP2) −185.60213, (4-31G–SCF) −187.90198, (MP2) −188.24422 au; HCOOH (STO-3G–SCF) −186.21245, (MP2) −186.36416, (4-31G–SCF) −188.47521, (MP2) −188.81602 au. For transition-state model (II),[29] the SCF energies are (STO-3G) −298.82989 and (4-31G) −302.64904 au.

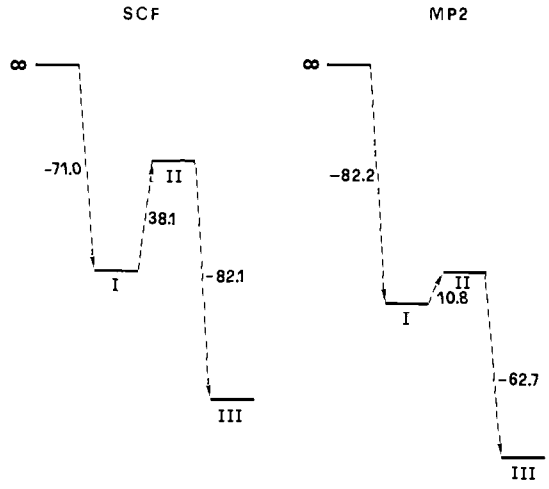

Figure 4. Relative SCF and MP2 energies on I, II, and III with NH_4^+ complexes to the DHAP at the STO-3G level, at 4-31G geometries.

in supplementary material Table VI.

The summary of the relative energies for models Ic, IIc, and IIIc at the SCF and MP2 levels using the 4-31G basis set are presented in Figure 2. The comparable results[16] at the STO-3G level with models Ib, IIb, and IIIb (R = CH_3) are presented in Figure 3. (The STO-3G results with R = H, models Ic–IIIc, showed that the effect of the methyl group on these relative energies was small.) Figures 2 and 3 make it clear that there is both a large energy difference and/or a large barrier between species I and III. The more reliable 4-31G basis set finds an energy difference between I and III of ~26 kcal/mol (SCF) and ~23 kcal/mol (MP2). These numbers are comparable to the difference in calculated proton affinities of $HCOO^-$ (360 kcal/mol, Table IV, calculated, compared to 342 kcal/mol, experimental[30,31]) and the enediolate ion (389 kcal/mol, Tables I and II). To confirm that these energies were not very sensitive to the C···O distances in our model, we carried out a further set of 4-31G calculations for models I, II, and III as a function of this distance. As one can see (Table VII), the numbers change somewhat upon geometry optimization, but it is clear that the intrinsic energy difference between species I and III is near 26 kcal/mol.

At this point, we cannot say whether our model for II represents a true transition state or is merely a point along the straight uphill pathway between I and III. But it is clear in any case that the intrinsic energy for the I → III is very unfavorable and completely inconsistent with a facile isomerization reaction. Thus, we turn to models to attempt to simulate the effect of the enzyme on the relative energies of species I and III.

Incorporation of Environment into the Calculations. Our first, very simple model was to include in the quantum mechanical calculation an NH_4^+ group (to simulate the presence of Lys 13), with an H^+···O=C (Ib) distance of 1.8 Å and an C=O···H^+ angle of 120°. The results of these calculations, at the STO-3G level, on I–III with NH_4^+ added, are shown in Figure 4. A comparison of Figure 3 with Figure 4 shows the dramatic effect that charged groups can have in stabilizing III relative to I. This led us to try to get a more realistic description of the "environmental effect" of TIM on the reaction. We thus model built a number of

Table VIII. Results of Molecular Mechanical Calculations on YTIM and Its Complexes

system	total refined energy, kcal/mol
YTIM–DHAP (I) (S1)[a]	−443.6
YTIM–DHAP (I) (S2)[a]	−464.1
YTIM–DHAP (I) (S3)[a]	−465.4
YTIM(His 95 → Gln)–DHAP (I)[b]	−470.8
YTIM (Glu 165 → GluH)–ENE (III)[c]	−488.3
YTIM[d]	−429.9
YTIM (His 95 → Gln)[e]	−436.8
YTIM (Glu 165 → GluH)[f]	−417.2
ENE (III)[g]	18.1
DHAP (I)[h]	−16.7
YTIM (Glu 165 → GluH, His 95 → Gln)–ENE (III)[i]	−543.3
YTIM (Glu 165 → GluH, His 95 → Gln)[j]	−446.5

[a] S1, S2, and S3 are three different model-built structures of yeast TIM with DHAP. Figure 5a,b shows S3. [b] Complex of YTIM with His 95 changed to Gln 95 and energy refined with DHAP (Figure 5d). [c] Complex of YTIM–enediolate in which proton has been transferred from DHAP → Glu 165 (Figure 5c). [d] YTIM energy refined without substrate. [e] YTIM with His 95 changed to Gln 95 and energy refined. [f] YTIM with Glu 165 protonated and energy refined. [g] Enediolate energy refined. [h] DHAP energy refined. [i] YTIM with His 95 → Gln 95, Glu 165 protonated, complexed with enediolate (Figure 5e). [j] YTIM with His 95 → Gln 95, and Glu 165 protonated.

structures of TIM prior to receiving a preprint from T. Alber and G. Petsko[4] and then subsequently refined a model that was built to simulate Figure 6a in that paper. This geometry of DHAP in the Alber and Petsko paper is based on difference density analysis of the yeast TIM–DHAP complex and the native enzyme. Encouragingly, the Alber/Petsko model-built geometry (S3) refines (Table VIII) to an energy lower than that of the other two structures (S1 and S2). We also carried out a number of other refinements, based on starting with the Alber/Petsko structure: first, we transferred the proton from DHAP to Glu 165 and energy refined that enediolate complex. We also replaced His 95 with Gln and energy refined that structure. Finally, we energy refined all three protein structures, by themselves as well as DHAP (I) and the enediolate (III). In Figure 5 we present a larger monopicture of the refined DHAP–TIM complex as well as stereopictures of the DHAP–TIM complex, the enediolate–$TIMH^+$ complex, and the corresponding complexes with "mutated TIM", in which His 95 has been replaced by a glutamine.[32] Interestingly, the replacement of His 95 with Gln and subsequent energy refinement lead to a new structure, discussed below, in which the Gln 95 hydrogen bonds to Glu 165.

Given the Alber/Petsko YTIM–DHAP complex, it is clear that His 95, Lys 13, and Glu 97 are the polar and ionic groups expected to most influence the isomerase reaction. We thus repeated the ab initio calculations represented in Figures 2 and 3 with various partial *charges* to represent the side chain of His, Lys, and Glu in the one-electron Hamiltonian. Both STO-3G and 4-31G models were studied, and the energies for these models are summarized in Table IX. At this point, we also considered the possible role of the phosphate group, representing it as a 2− charge placed at the center of the three oxygens in the molecular mechanics optimized model of the YTIM–DHAP complex or as a 2−/2+ ion pair, with the 2+ charge 2 Å from the 2− charge along the threefold PO_3^{2-} axis. One cannot argue that either of these is a particularly realistic way to simulate the role of the phosphate, but it should give us a qualitative idea of what the effect of such a group might be. We also carried out such quantum mechanical

(29) We studied the $[HO\cdots H\cdots CHOHCHO]^-$ complex, keeping O···C fixed at 3.4 Å and O···H at 1.7 Å, but optimizing some of the internal geometry of the "enediolate" part of the molecule. This optimization, carried out at the 4-31G level, led to a model transition-state geometry reported in Table VI (total energies; see ref 28). We then repeated the calculations using these optimized geometrical parameters for the enediolate portion of the transition state, replacing OH^- with $HCOO^-$ and using its 4-31G optimized geometries for $HCOO^-$ and HCOOH complexes (Ic and IIIc) with a linearly interpolated geometry for the transition state $HCOO^-\cdots H\cdots$IIc.

(30) Yamdagni, R.; Kebarle, P. *J. Am. Chem. Soc.* **1973**, *95*, 4050.

(31) An extensive comparison of 4-31G calculated and experimental proton affinities is in: Kollman, P.; Rothenberg, S. *J. Am. Chem. Soc.* **1977**, *99*, 1333.

(32) The TIM residues included in the calculation were Asn 10, Lys 13, His 95, Ser 96, Glu 97, Arg 98, Cys 126, Glu 129, Tyr 164, Glu 165, Pro 166, Val 167, Trp 168, Ala 169, Ile 170, Ala 171, Tyr 208, Gly 209, Gly 210, Ser 211, Ala 212, Leu 230, Gly 232, Gly 233, Ala 373, Phe 374, Thr 375 (these latter three from the second TIM molecule, the molecule being present in the crystal as a dimer).

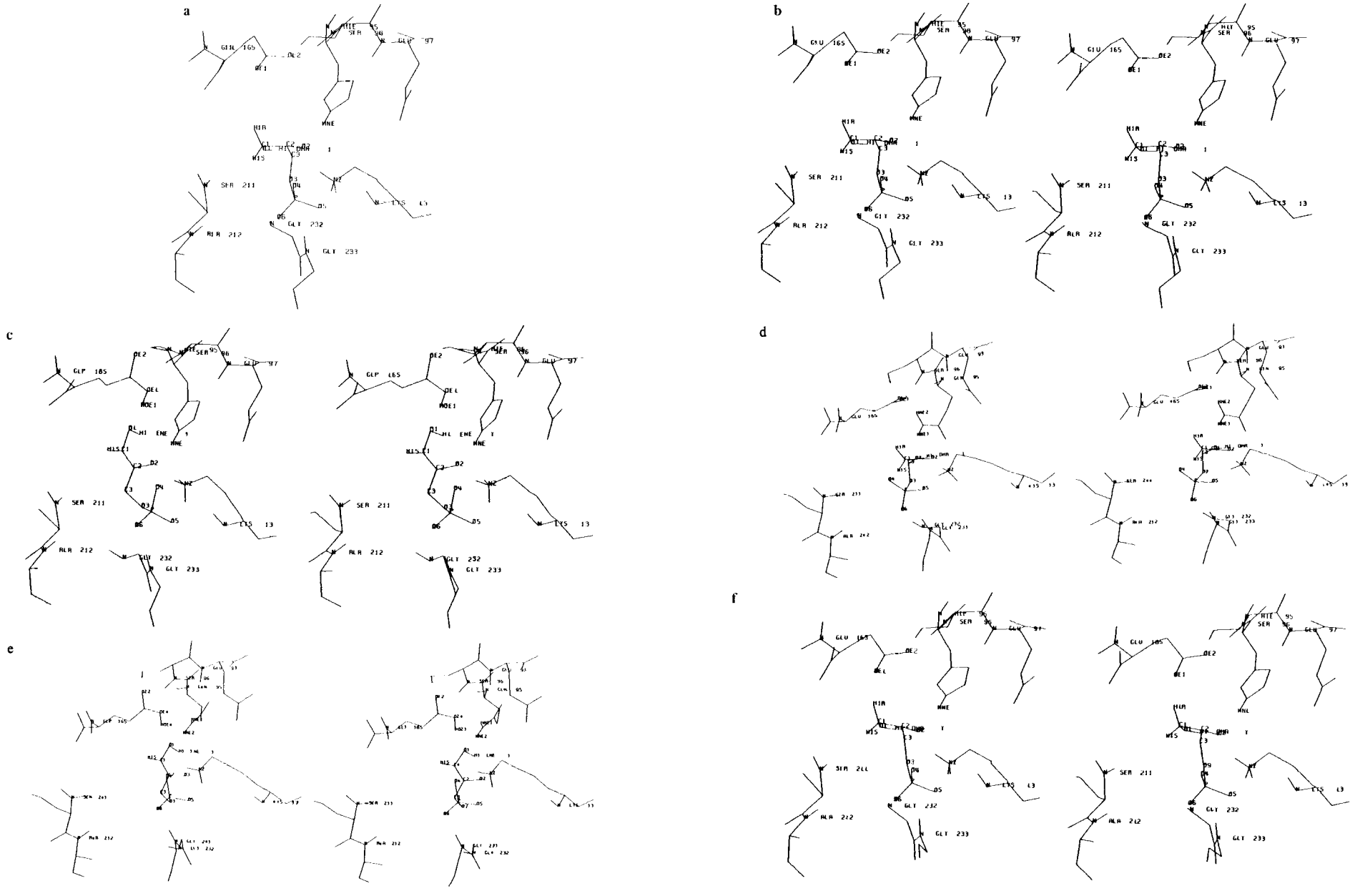

Figure 5. Mono- (a) and stereoview (b) of yeast TIM–DHAP complex; and stereoviews of (c) yeast $TIMH^+$–enediolate complex, (d) yeast TIM (His 95 → Gln 95)–DHAP complex, (e) yeast $TIMH^+$ (His 95 → Gln 95)–enediolate complex, and (f) yeast TIM–DHAP complex forcing C···O distance to be 3.0 Å with C_α constraint 10 kcal/(mol Å^2) (see ref 35). See ref 32 for a list of all residues included in the calculation. Here we only display the energy-refined structure of the residues displayed by Alber and Petsko (ref 4) in Figure 6a of their *Biochemistry* paper.

Table IX. Effect of Environment and Correlation Energy on the Relative Energy of I, II, and III (kcal/mol)

complex	SCF[a]	MP2[b]	H[c]	L[d]	L, G[e]	H, L, G[f]	H, L, G, P[g]	G, L, G, P[h]	G, L, G, P[i]	H, L, G[k] (MP2)
					STO-3G Basis Set					
Ib	−6.9	−19.5	−10.1	−55.9	−26.2	−30.0	−13.7	−29.2	−12.7	0
IIb	49.3	15.1	43.7	−10.9	23.7	17.2	43.0	19.1	44.9	25.6
IIIb	7.3	−4.9	−3.4	−76.2	−32.8	−44.2	−4.5	−40.4	−0.6	−13.8
					4-31G Basis Set					
Ib	−14.0 (−13.8)[j]	(−13.9)[j]				−45.9	−34.3	−44.2	−32.3	0
IIb	35.7 (32.7)[j]	(18.6)[j]				−3.6	15.5	−0.9	18.4	28.3
IIIb	17.9 (11.9)[j]	(8.8)[j]				−40.5	−7.5	−35.9	−2.7	2.4

[a] Relative energies at the SCF level relative to separated $HCOO^-$ and DHAP model. [b] Including Môller Plesset (MP2) correlation correction.[33] [c] SCF calculation with the inclusion of His 95 charges. [d] SCF calculation with Lys 13 charges. [e] SCF calculation with Lys 13 and Glu 97 charges. [f] SCF calculation with His 95, Lys 13, and Glu 97 charges. [g] SCF calculation with His 95, Lys 13, Glu 97 charges; P stands for PO_4^{2-} represented as a dipole 2−/2+; see text). [h] The same as *f*, but with His 95 replaced by Gln. [i] The same as *g*, but with His 95 replaced by Gln. [j] The values in parentheses refer to calculations on model system (R = H) (Ic, IIc, IIIc). [k] Relative energies estimated after accounting for both MP2 correction to SCF and the environmental effect of His 95, Lys 13, and Glu 97 (H,L,G model) at the 4-31G level; we estimated the MP2 correction by using the energies in parentheses.

calculations on Gln replacing His 95 *but* assuming that the Gln is in a similar location as His, in contrast to what we subsequently found in the molecular mechanics refinement. Given the uncertainties in our refinement model, this seemed a sensible thing to do. As we noted above, the role of the enzyme is to stabilize the enediolate anion/COOH (III) relative to DHAP/COO^- (I), and the molecular mechanical energies in Table VIII support that it is doing this, in that the reaction YTIM–DHAP → YTIM$^+$ (Glu 165 → Glu 165 H^+)–ENE is calculated to be energetically favored by 23 kcal/mol. Given that the gas-phase energy difference between the Ib and IIIb species (estimated at the MP2 level) is ~27 kcal/mol, we see that the enzyme is doing exactly what one would expect. The quantum mechanical calculations including the partial charges have led to a similar conclusion, if we consider the charges of His 95, Lys 13, and Glu 97 as the most appropriate model. For example, at the STO-3G level (Table IX), the H, L, G model suggests that the enzyme stabilizes III relative to I by 28.4 kcal/mol, and at 4-31G, the corresponding difference is 26.5 kcal/mol. However, the inclusion of the charge of the "phosphate ion pair" in the quantum mechanical calculation significantly destabilizes III, relative to I, as one might expect since the anionic charge in I → III goes closer to the phosphate. What is interesting is that in the molecular mechanical simulation, the phosphate is represented as a *nonneutralized* dianion and enzyme still stabilizes III relative to I.

Proton-Transfer Barriers. Now that we have shown how the enzyme stabilizes III relative to I, so that these species become approximately of equal energy, we turn to the energy of II and the activation energy for the process I → II → III. For the TIM reaction to be as fast as it is, this energy barrier should be in the range of 15 kcal/mol or lower. From Table IX, it is clear that inclusion of correlation energy (MP2 level) is crucial in representing this barrier realistically, in that it stabilizes II relative to I and III by about 20 (STO-3G level) and 14 kcal/mol (4-31G level). If one adds these numbers to the H, L, G model values in Table IX, one sees that the proton-transfer barrier is ~26–28 kcal/mol at either STO-3G or 4-31G, still unrealistically high (see the last column of the table). However, we should recall, as discussed above, that we used C···O distances of 3.53–3.29 Å to model I–III. Given the complexity of optimizing both the C···O distance and the enzyme orientation, we turned to a simpler model for this proton-transfer process which could *mimic* our I → II → III reaction, but with the energy of the two ends states approximately equal, as if the environment of the enzyme were there. A simple isosteric analogue to C–H···O was N–H···N, so we turned to the very simple model H_3NH^+···NH_3, where the calculation of the proton-transfer pathway should be quite straightforward, and examined the energy for this model with the proton at 1.0 Å from one N and equidistant from the nitrogens. The proton-transfer energetics for this model and the results are summarized in Table X. As one can see, the proton-transfer barrier is substantial (~25 kcal/mol) at R(N–N) = 3.4 Å but is lowered considerably to ~15 kcal/mol at R(N–N) = 3.2 Å. We compared the energy for the proton-centered and normal asymmetric structures with a 6-31G** basis set at the SCF and MP2 levels and with a 4-31G basis set at the SCF, MP2, MP3, CID, and CID(SC) levels.[33] The results (Table X) show that a 4-31G/MP2 model gives qualitatively reasonable results, not greatly different from either 4-31G/CID or 6-31G**/MP2. Furthermore, the barriers for N···H···N^+ proton transfer at 3.4 Å are close to those found in our more complex C···H···O systems (using the 4-31G model with H, L, G charges and adding the MP2 correction in parentheses for I vs. II lead to an energy estimate (Table IX) of 28.3 kcal/mol). We examined the proton-transfer barrier for an N···N distance of 3.2 Å at the 4-31G/SCF, -MP3, and -CID levels of theory, and the proton-transfer barrier is now ~15 kcal/mol, very close to the value calculated by Harding and Scheiner[34] at this N···N distance. The agreement between our two sets of calculations is encouraging and supports the reasonableness of our values for the N···N and C···O proton-transfer energies at 3.4 Å. The proton-transfer barriers are clearly most highly sensitive to heavy-atom separation, as has been noted previously.[34]

Table X. Effect of Correlation Energy and N···N Distance on the Proton-Transfer Barrier in H_3N···H···NH_3^+

R(N···N)[a]	basis set	barrier[b] SCF[c]	MP2[d]	MP3[e]	CID[f]	CID (SC)[g]
3.4	4-31G	33.99	23.67	25.87	27.41	25.38
3.4	6-31G**	38.25	28.72			
3.2	4-31G	22.64	14.13	16.00	17.23	15.63
3.0	4-31G	12.12	5.28	6.83	7.77	6.56
2.9	4-31G	7.74	1.79	3.19	3.98	2.98

[a] Angstroms. [b] Values in kcal/mol. [c] Relative energy of complex of NH_4^+···NH_3 with all angles tetrahedral and all N–H distances 1.0 Å and a symmetric structure with all internal distanes the same at the SCF level. [d] Same as *c* at the MP2 (second-order Môller Plesset) level[33] of theory. [e] Same as *c* at the MP3 (third-order Môller Plesset) level of theory. [f] Same as *c* at the CID (configuration interaction including all double excitation) level of theory. [g] Same as *c* at the CID (SC) (configuration interaction including all double excitations and size consistent) level of theory.

Thus, we can see that the barrier for the process I → II → III can be quite small, as long as the C···O (N···N) distance is <3.2 Å. As shown in Table X, the estimated proton-transfer barrier at the highest level of theory is ~7 kcal/mol at R(C···O) = 3.0 Å and 3 kcal/mol at R(C···O) = 2.9 Å. However, the question remains: can the enzyme achieve such short C···O distances without large strain energy in the rest of the structure? As one can see (Figure 5a,b), the *minimum* energy structure of the en-

(33) Binkley, J. S.; Pople, J. A. *Int. J. Quantum Chem.* **1975**, *9*, 229.
(34) Scheiner, S.; Harding, L. *J. Am. Chem. Soc.* **1981**, *103*, 2169.

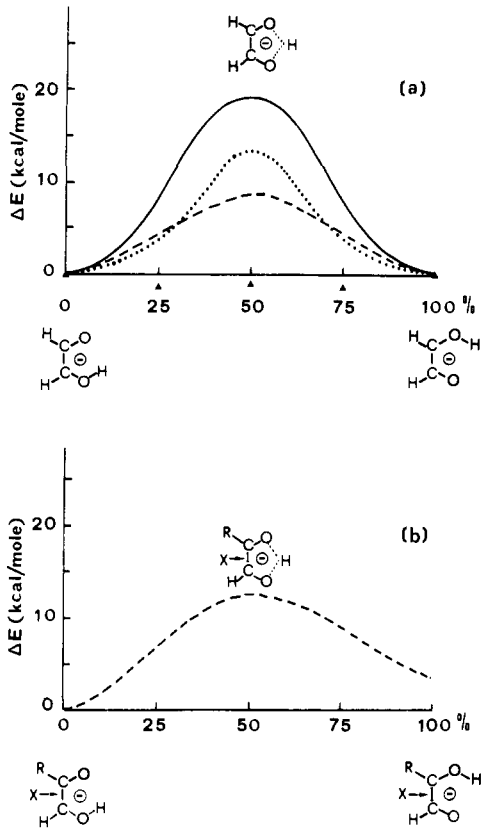

Figure 6. (a) Relative energy for proton transfer in IV, with interpolated geometries at 25% and 75% proton transfer: (full line 4-31G; (dashed line) STO-3G; (dotted line) 4-31G/MP2. (b) Relative STO-3G SCF energy for proton transfer in IV, R = CH_3, with X = HCOOH.

zyme–DHAP complex has a C···O distance nearer 4.0 Å. We thus carried out further molecular mechanical calculations on TIM–DHAP, in which we forced the C···O distance to be 3.0 and 2.9 Å and the H···O distance 1.91 and 1.81 Å, to simulate the transition-state geometry (II) (Figure 5f). In the analysis of such calculations we factored out the molecular mechanical energy associated with the COO^-···HCHOH–C(O)– fragment, since it is included in the quantum mechanical energies. The remaining "strain" energy in the comparison of the unconstrained and constrained TIM–DHAP complex was calculated to be ~1.5–7.1 kcal/mol at 3.0 Å and 1.6–7.3 kcal/mol at 2.9 Å. Thus, we estimate the proton-transfer barriers as follows: using the relative energies in Table VII, we note that it costs ~0.5 kcal/mol (3.0 Å) and 1.2 kcal/mol (2.9 Å) to force the C···O distances to be 3.0 and 2.9 Å, respectively. At these distances the enzyme strain energies are 1.5–7.1 (3.0 Å) and 1.6–7.3 kcal/mol (2.9 Å).[35] Finally, the intrinsic barriers to proton transfer at these distances are 7.0 kcal/mol (3.0 Å) and 3.0 kcal/mol at 2.9 Å. This leads to estimated proton-transfer barriers of 9–15 kcal/mol (3.0 Å) and 6–12 kcal/mol (2.9 Å), respectively.

Proton-Transfer Steps 3 and 4. Next, we examined steps 3–4 in the reaction, proton transfer within the enediolate anion under the possible influence of the location of HCOOH. The proton transfer between the two oxygens (O_1 and O_2) of the enediolate, after 4-31G optimization of the models for the asymmetric enediolate model and a model for half-proton transfer, is described in supplementary material Table XI. Figure 6a shows the barrier for this proton transfer at 4-31G SCF and MP2 levels; also the STO-3G values for the same geometry as 4-31G are reported. We have also computed the barrier with HOH interacting with one of the C atoms or the center of the bond C–C. Because of the small difference among the energies in the various positions, we chose the middle position, corresponding to the intermediate energy, to do the calculations on the system HCOOH···enediolate (IVb) shown in Figure 6b.

As one can see from Figure 6, the barrier to proton transfer at the highest level of theory is ~14 kcal/mol.

We did not carry out any explicit quantum mechanical calculations on steps 5 and 6 (structures V, VI, and VII) since, by inference, the electronic structure changes in these steps are essentially the reverse of steps 1 and 2.

Discussion

Above, we have shown that the intrinsic energy for the DHAP proton abstraction by $-COO^-$ is an uphill process and the crucial role of the enzyme is in making this proton abstraction facile. In particular, our calculations have shown how TIM stabilizes the enediolate intermediate with Glu 165 protonated relative to DHAP and Glu 165 anion by about 25 kcal/mol if one uses the molecular mechanical model, or the quantum mechanical model without phosphate. It is clear from the quantum mechanical calculations that both His 95 and the Lys 13–Glu 97 ion pair are important in this stabilization. Since our model calculations used R = CH_3 or H instead of R = $CH_2OPO_3^{2-}$ for I and II, we sought to evaluate the effect of including the electrostatic effect of the phosphate. The inclusion of a 2– charge or a 2–/2+ dipole in the quantum mechanical calculations in order to represent the phosphate group with a gas-phase dielectric constant (ϵ = 1) completely counteracts the stabilization of III by His, Lys, and Glu. In the molecular mechanical calculations, however, the phosphate was included explicitly *without* counterion and a distance-dependent dielectric was used ($\epsilon = R$). Furthermore, we did not "solvate" the phosphate with the flexible loop (residues 168–177), known[4] to move to interact more effectively with the phosphate. In view of this, it was extremely encouraging to us that the stabilization of III relative to I was ~25 kcal/mol, close to what the quantum mechanical model (sans phosphate) gave. In our opinion, we are treating the highly charged phosphate more realistically in the latter case, and, thus, are getting more realistic results from its inclusion in the calculation.

Another way of viewing the enzyme *polarization* of the substrate is to evaluate the electrostatic potential at the substrate atoms due to the enzyme. We have carried out such a calculation on a chicken muscle TIM/DHAP complex[36] and find that all of the atoms of DHAP except for the *pro-R* hydrogen at C1 are in a region of positive potential; the *pro-R* hydrogen is in a negative potential region due mainly to Glu 165. This gives a beautiful qualitative picture on the facilitation of the proton abstraction reaction by the enzyme.

Given the clear stabilization of III relative to I by TIM, how relevant is this to the enzyme reaction, since Rose et al.[6] argue strongly that it is the enediol (O–H protonated version of III) which is the intermediate in the enzyme and in solution for the isomerization of I. On the other hand, the effectiveness of phosphoglycolate[37] and phosphoglycohydroxamate[38] as inhibitors of TIM argues for an important role of the enediolate at some stage of the catalytic pathway. Although the theoretical methods to accurately assess this possibility are not available, we should note that an enediol intermediate is not necessarily incompatible with what has been calculated here. Knowles et al.[1] have found significant (85%) isotopic scrambling of the proton which is

(35) In these calculations, we factored out the molecular-mechanical energies for the COO^- group of Glu 165 and the CH_2OHCO part of DHAP, since we are including their energies in the quantum-mechanical calculation. With a 10 kcal/mol constraint on all backbone Cα's, the energy difference between the results of the calculation shown in Figure 5b and that where we force the Glu 165 OE1···DHAP H1R distance to be 1.91 Å and the Glu 165 OE1···DHAP C1 distance to be 3.00 Å with a harmonic restraint function of 100 kcal/(mol Å^2) is 7.1 kcal/mol; if the backbone Cα constraint is only 1 kcal/mol, this energy difference is only 1.5 kcal/mol. Since the X-ray coordinates for TIM and its complex are at not very high resolution, it is not clear which is the more realistic model. The corresponding strain energies when C···O is 2.9 Å and H···O is 1.81 Å are 1.6 and 7.3 kcal/mol, respectively.

(36) Unpublished calculations by PAK based on model-built coordinates on he DHAP/chicken muscle TIM complex at Oxford (courtesy of D. Phillips and G. Petsko).

(37) Wolfenden, R. *Nature (London)* **1969**, *223*, 704.

(38) Collins, K. *J. Biol. Chem.* **1974**, *249*, 136.

transferred from C_1 to C_2, suggesting some accessibility (which could be rather transient) of H_2O to the active site. Once the enediolate is formed, some penetration of water into the active site could easily protonate the enediolate in a process with a very low activation energy. One of the roles of TIM is apparently to protect the enediol from phosphatase action, but the amount of water "penetration" to attack the enediol and displace the phosphate is likely to be much more than required to protonate the enediolate. In summary, our calculations suggest that the enzyme sufficiently stabilizes the enediolate that, even if enediol is the ultimate intermediate, proton abstraction from DHAP does not have to occur in a concerted fashion with protonation of the enediolate.

Once the stability of the enediolate is brought down to the same level as that of DHAP by the enzyme, proton transfer is not totally uphill and the barrier to proton transfer can be considered. One of the intriguing results of our calculations is the very similar proton-transfer barrier we calculate for R(C···O) at 3.4 Å after considering His, Glu, and Lys charges and the MP2 correction (28.3 kcal/mol) and the barrier we calculate for H_3N^+–H···NH_3 at R(N···N) 3.4 Å with 6-31G** MP2 (28.7 kcal/mol). Both of these barriers are clearly too high for a facile reaction. However, there is significant precedent in the literature[34] that X···H···Y proton-transfer barriers, where X, Y = N, O, F, are much more dependent on R(X···Y) than on the nature of X and Y. This, and the similarity in the barrier calculated for II and the $N_2H_7^+$ model, lets us use that model at shorter N···N distances; the distance only 0.2 Å less decreases the barrier to ~15 kcal/mol and, at N···N distance of 3.0 Å, Scheiner and Harding[34] and we have shown that the barrier is only ~7–8 kcal/mol; at 2.9 Å, we calculate the barriers to be ~3 kcal/mol. The correspondence between C···O and N···N barriers at the same distance between heavy atoms allows us to infer that, if R(C–H···O^-) is ~3.0 Å in the enzyme active site, facile proton transfer will occur. Adding our quantum mechanical energies for proton transfer to our molecular mechanical strain estimates leads to a calculated barrier for the proton-transfer step of I → III in the range of 6–14 kcal/mol. These do not consider the likely rate enhancement due to tunneling effects. Although we cannot *prove* that such a short C···O distance occurs in TIM, it certainly is plausible, given the molecular mechanics refined energies and geometries (Figure 5f) and the results in Table VII, in which we show that the energy difference is very small in the range of R(C–H···O) from 3.4 to 2.9 Å, at which point the proton-transfer barrier would be very small.

Once the enediolate (III) has been formed, our calculations on the O–H···O proton transfer within the enediolate (Figure 6) show that it is also facile (steps 3 and 4 of the reaction scheme), although steps 3 and 4 are not relevant if the intermediate is an enediol. However, in either case, the reverse proton transfer from Glu 165 can take place to C_2 of the enediol(ate) (steps 5 and 6) with the reverse of the process of steps I → III. The interesting question remains how the enzyme causes the proton to be delivered back to C_2 rather than C_1. This could be accomplished by small movements of either His 95 or Lys 13, which would stabilize the O–H proton on O_2 rather than O_1 of the enediol(ate). In addition, if the intermediate is enediolate, a small motion of either of these groups to less effectively stabilize the enediolate would make the proton transfer back from Glu 165 an almost downhill process.

We are continuing our studies to further understand how the enzyme might preferentially stabilize GAP over DHAP, since it appears that the equilibrium constant for these species on the enzyme is ~1, quite different from the solution value favoring DHAP by ~10^2–10^3,[1,6] although this difference has not been unequivocally established.

TIM increases the rate for this isomerization reaction by 10^9 such that product dissociation becomes rate limiting. It appears from the kinetic work by Rose[6] that the rate-limiting step for the reaction is an enzyme conformational charge, which, the X-ray studies of Alber and Petsko suggest,[4] would be the opening of the flexible loop (residues 168–177) which closes to bind the phosphate group of the substrate. Our focus in this paper has been to show how the enzyme reduces the activation energy for the *chemical* steps, such that the enzyme conformational change becomes rate limiting. Our calculated stabilization energy for the enediolate at the molecular mechanics level of 23 kcal/mol is still larger than the estimated 3×10^9 (ΔG = 13 kcal/mol) for enzymatic rate enhancement.[5] However, in addition to the simplicity of our model, we should note that 10^9 might be a lower bound for the decrease in activation energy for the *chemical* steps of the reaction.

Recombinant DNA techniques offer a very exciting prospect for understanding enzyme catalysts as well as *designing* new enzymes. Davenport and Petsko[7] have worked on replacing His 95 with Gln. The rationale behind this was that Gln could also act as an H-bond proton donor and acceptor, like His, but because of its much larger pK_a, cannot act as a general acid. Thus, the necessity of a general acid in the catalyst could be assessed. Our quantum mechanical calculations using Gln charges instead of His suggest indeed that, electrostatically, Gln 95 can stabilize the enediolate similarly to His 95. However, in our molecular mechanics refinement of TIM (His 95 → Gln) with DHAP, we find that Gln 95 moved to a location different from His 95 and formed an H bond with Glu 165 (compare parts b and d, Figure 5). Thus, this amino acid substitution could also reduce the catalytic rate relative to native TIM *not* because of the loss of the acid catalytic function of His but rather because Gln 95 is more able to move and inhibit the proton abstraction by Glu 165 than is His 95 or because Gln 95 is more flexible than His 95 and moves from the position where it can aid proton abstraction by Glu 165. The above molecular mechanical results must be viewed with considerable skepticism because of the simplicity of the potential function/lack of inclusion of solvent. But they are intriguing in that they suggest a *possible* different result of the His → Gln mutant than one had anticipated. Whether the above conformation occurs in practive must await experimental studies on the mutant enzyme. It also should be emphasized that this H-bonded configuration Gln 95···Glu 165 may reduce the proton abstraction ability of Glu 165 and still not affect the enzymatic efficiency, if the rate-limiting step remains product dissociation from the enzyme. As a final caveat, we should note that the difference in energy between mutant TIM/DHAP and its enediolate is calculated to be −543.3 − (−470.8) = −72.5 kcal/mol, even larger than for native TIM. Thus, if mutant TIM can surmount the barrier caused by the possible Glu 165···Gln 95 H bond, it clearly can stabilize the enediolate very effectively.

Conclusion

We have presented quantum and molecular mechanical studies on models for the catalysis of the dihydroxyacetone phosphate–glyceraldehyde phosphate isomerization by the enzyme triosephosphate isomerase. The calculations suggest that the large rate enhancement due to TIM comes from a stabilization of the enediolate, which may be a true intermediate, or only on the pathway to an enediol. Both His 95 and Lys 13 contribute to this stabilization, and we cannot say which of these two is the "polarizing electrophile" noted by Belasco and Knowles. Once the DHAP and enediolate are of comparable energy, our calculations on models show that the proton-transfer barrier between DHAP or GAP and the enediolate should be very small as long as the C···O distance is ≤3.0 Å. Since the calculated minimum energy C···O distance in $HCOO^-$···DHAP (Ic) is calculated to be 3.15 Å, this distance is easy to achieve. Furthermore, the O–H···O proton transfer in the enediolate is also calculated to be small (10–15 kcal/mol). The enzymatic rate is then determined by product dissociation from the enzyme, which is presumably controlled by the rate of "loop opening" of residues 168–177.

Our preliminary calculations on a mutant TIM, in which His 95 is replaced by Gln 95, are interesting in that they have shown a possible consequence of the His 95–Gln 95 conversion (Gln 95–Glu 165 H bonding) which could greatly slow the rate of chemical catalysis, such that it could become rate limiting. This is a relatively rare example where a qualitatively new idea has emerged from molecular mechanics simulations, and we expect that such simulations may prove valuable in analyzing possible mutants on proteins whose crystal structure is known. Such

simulations are not accurate enough as yet to predict with confidence the consequences of protein replacement, but they may well be valuable in suggesting which mutations may have the most interesting consequences on enzyme catalysis and ligand binding.

Acknowledgment. We are grateful for the support of the NIH (GM-29072) in this work. This work was greatly aided by the receipt of yeast TIM coordinates from G. Petsko, by the receipt of preprints from T. Alber and G. Petsko which greatly aided the model building of the TIM-DHAP complex, and by stimulating conversations with Alber and Petsko. One of us (P.A.K.) thanks Prof. D. C. Phillips of the Oxford Molecular Biophysics Lab for stimulating his interest in TIM while P.A.K. was on sabbatical at Oxford in 1978-79. We also gratefully acknowledge the facilities of the Computer Graphics Lab supported by NIH-RR-1081, R. Langridge, and T. Ferrin, system manager, which was essential to this research.

Registry No. Ia, 57-04-5; Ib, 116-09-6; Ic, 141-46-8; IIIa, 89999-77-9; IIIb, 7333-03-1; IIIc, 1571-60-4; VIIb, 598-35-6; TIM, 9023-78-3; formic acid, 64-18-6.

Supplementary Material Available: Listings of structures and energies for α-hydroxyacetone, its enediolate anion, and glyceraldehyde 3-phosphate (Tables I-III), 4-31G geometry and corresponding energies at the STO-3G and 4-31G levels of $HCOO^-$ and HCOOH (Table IV), model calculations on anion-neutral complexes (Table V), transition-state II geometry at the 4-31G level (Table VII), and geometries for structures III and V and for transition-state IV at the 4-31G level (Table XI) (7 pages). Ordering information is given on any current masthead page.

Vinyl Mobility in Myoglobin as Studied by Time-Dependent Nuclear Overhauser Effect Measurements

S. Ramaprasad, Robert D. Johnson,[1] and Gerd N. La Mar*

Contribution from the Department of Chemistry, University of California, Davis, California 95616. *Received July 28, 1983*

Abstract: Nuclear overhauser effect experiments were performed on the protons of the 2-vinyl group in metcyanomyoglobin. Truncated NOE data were presented, with the observed cross-relaxation rate showing significant vinyl mobility relative to the heme. Good agreement between the selective T_1 rate was found for the 2-H(cis) vinyl resonance, and the effect of cross relaxation on the nonselective T_1 rate is discussed.

The vinyl substituents on the ubiquitous protoheme (A), found as the prosthetic group in myoglobins, hemoglobins, as well as several other classes of hemoproteins,[2] have been implicated in a number of functional roles. In the cases of the oxygen-binding proteins, variable vinyl interactions with the protein have been invoked to account for the Bohr effect in monomeric hemoglobin[3] and have been proposed to play a crucial role in the mechanism of cooperativity in human hemoglobin.[4,5] Interactions between the protein and the heme periphery influence both the equilibrium orientation and the oscillatory mobility of the vinyl group relative to the heme plane. While single-crystal X-ray studies have sometimes differentiated between rotationally locked and rotationally disordered vinyl groups,[6] they generally provide no direct information on the dynamics of this side chain. It can be expected that the oscillatory mobility of the vinyl group will provide a very sensitive probe of heme-protein interactions.

We have been interested in determining by solution NMR methods both the equilibrium orientation and the rotational mobility of heme side chains and the relationship of these properties to protein function. As a model we have selected sperm whale myoglobin in the metcyano form for the initial studies. This protein has been crystallographically characterized in many forms.[6-8] Extensive deuteration studies have provided unequivocal assignment of many of the hyperfine shifted heme resonances in the ^1H NMR spectrum, including all three protons of the 2-vinyl group.[9,10]

Two NMR methods appear particularly attractive for characterizing the internal motion of heme substituents. It has been shown elsewhere that ^2H NMR relaxation data of isotope-labeled vinyl and propionate side chains can be analyzed in terms of the internal motions.[11,12] Although it is generally thought that paramagnetically shifted or relaxed protons do not exhibit a nuclear Overhauser effect, NOE, because of the sizable paramagnetic "leakage", several cases have been found where cross relaxation, and hence NOEs, contribute significantly to the overall relaxation rate of protons in the heme cavity of a paramagnetic hemoprotein.[13,14] Cross relaxation is also manifested in the curvature of semilogarithmic plots of spin-lattice relaxation experiments,[15] but it can be measured more effectively through the NOE.

The basic NOE experiment is to saturate a specific NMR resonance and observe resultant intensity changes in other resonances that occur through cross relaxation.[16] As the strength

(1) Present address, IBM Instruments, Orchard Park, Danbury, CT 08610.
(2) Antonini, E.; Brunori, M. "Hemoglobin and Myoglobin in their Reactions with Ligands", American Elsevier Publishing Co.: New York, 1971; Chapters 4 and 13.
(3) La Mar, G. N.; Viscio, D. B., Gersonde, K.; Sick, H. *Biochemistry* **1978**, *17*, 361.
(4) Gelin, B. R.; Karplus, M. *Proc. Natl. Acad. Sci. U.S.A.* **1977**, 801.
(5) Perutz, M. F. *Br. Med. Bull* **1976**, *32*, 195.
(6) Seybert, D. W.; Moffat, K. *J. Mol. Biol.* **1976**, *106*, 895.
(7) Takano, T. *J. Mol. Biol.* **1977**, *110*, 537.
(8) Phillips, S. E. V. *J. Mol. Biol.* **1980**, *142*, 531.
(9) Krishnamoorthi, R. Ph.D. Dissertation, University of California, Davis, CA, 1983.
(10) Sheard, B.; Yamane, T.; Shulman, R. G. *J. Mol. Biol.* **1970**, *53*, 35.
(11) Johnson, R. D.; La Mar, G. N., submitted for publication; La Jolla Symposium on Protein and Nucleic Acid Structure and Dynamics, La Jolla, CA, September 1982, Abstracts.
(12) Lee, R. W. K.; Oldfield, E. *J. Mol. Biol.* **1982**, *257*, 5023.
(13) Trewhella, J.; Wright, P.; Appleby, C. A. *Nature (London)* **1980**, *280*, 87-88.
(14) La Mar, G. N.; Ramaprasad, S.; McLachlan, S., unpublished results.
(15) Sletten E.; Jackson, J. T.; Burns, P. D.; La Mar, G. N. *J. Magn. Reson.* **1983**, *52*, 492.
(16) Noggle, J. H.; Shirmer, R. E. "The Nuclear Overhauser Effect"; Academic Press: New York, 1971.

0002-7863/84/1506-3632$01.50/0